PHYSICAL REVIEW D **86,** 036011 (2012)

$W_L W_L$ scattering at the LHC: Improving the selection criteria

Krzysztof Doroba,[1] Jan Kalinowski,[1,2] Jakub Kuczmarski,[1] Stefan Pokorski,[1] Janusz Rosiek,[1]
Michał Szleper,[3] and Sławomir Tkaczyk[4]

[1]*Physics Department, University of Warsaw, Hoża 69, 00-681 Warsaw, Poland*
[2]*University of Hamburg, Luruper Chaussee 149, D-22761 Hamburg, Germany, and DESY, Notkestrasse 85, D-22607 Hamburg, Germany*
[3]*National Center for Nuclear Research, High Energy Physics Department, Hoża 69, 00-681 Warszawa, Poland*
[4]*Fermi National Accelerator Laboratory, Batavia, Illinois 60510, USA*

(Received 21 March 2012; published 27 August 2012)

We present a systematic study of the different mechanisms leading to WW pair production at the Large Hadron Collider (LHC), both in the same-sign and opposite-sign channels, and we emphasize that the former offers much better potential for investigating non-resonant $W_L W_L$ scattering. We propose a new kinematic variable to isolate the $W_L W_L$ scattering component in same-sign WW production at the LHC. Focusing on purely leptonic W decay channels, we show that it considerably improves the LHC capabilities to shed light on the electroweak symmetry breaking mechanism after collecting 100 fb^{-1} of data at $\sqrt{s} = 14$ TeV. The new variable is less effective in the opposite-sign WW channel due to different background composition.

DOI: 10.1103/PhysRevD.86.036011 PACS numbers: 14.70.Fm, 11.15.Ex, 13.38.Be

I. INTRODUCTION

The longitudinal WW scattering carries the most direct information about the mechanism of electroweak symmetry breaking, no matter whether a physical elementary Higgs particle exists or some kind of strongly interacting physics is responsible for this breaking. In fact, even if a light Higgs boson is discovered, the energy dependence of the longitudinal WW scattering above the Higgs mass scale will tell us if the Higgs boson unitarizes the WW scattering fully or only partially, as in some theoretical models with composite Higgs [1]. Experimental investigation of the $W_L W_L$ scattering as a function of its center-of-mass energy M_{WW} becomes feasible at the Large Hadron Collider (LHC). The techniques for observing the $W_L W_L$ scattering signal in pp collisions have been extensively investigated and reported in many papers [2–11]. These techniques are based on the differences in the emission process of the transverse and longitudinal gauge bosons from the colliding quarks and in the behavior of the respective WW scattering amplitudes as a function of their center-of-mass energy and the scattering angle. These effects are, however, strongly masked by the quark distribution functions inside the proton and by various sources of large background. It has been found that techniques such as forward jet tagging, central jet vetoing, and cuts on the final lepton transverse momenta are very promising in the isolation of the $W_L W_L$ scattering signal from the background. At the same time, the above studies clearly show that such measurement would be experimentally very challenging and typically require at least a year to several years of LHC running at full nominal parameters to obtain observable effects. In view of this, possible new techniques allowing for better event selection and better data analysis can play an important role in making the study feasible in a relatively shorter time scale.

Given the importance of the experimental access to the longitudinal WW scattering channel, we readdress this issue in the present paper. We search for the most efficient event-selection criteria for observing a signal of an enhanced, compared to the prediction of the Standard Model (SM) with a light Higgs boson, $W_L W_L$ scattering at the LHC running at an energy of 7, 8, and 14 TeV. Such an enhancement can exist because the SM Higgs boson is heavy or a light Higgs boson has modified couplings compared to the SM, so that it does not fully unitarize the $W_L W_L$ scattering (see, e.g., [12]), or because there is no physical Higgs boson at all. The magnitude of the enhancement and its detectability would, of course, depend on its origin. It is not the purpose of this paper to compare these different theoretical scenarios but merely to find an improvement in the selection of the $W_L W_L$ scattering signal. Therefore, in our search for the best signal, we choose the Higgsless scenario for our hypothetical enhanced $W_L W_L$ scattering, which gives the strongest but still physically realistic enhancement compared to the SM prediction with a light Higgs boson in which the effects of our new event selection criteria are most visible. Based on our study, we propose a new kinematic variable for the longitudinal W^+W^+ scattering signal, showing that it gives significant improvement of the signal-to-background (S/B) figures compared to all the previously discussed selection criteria applied to the same hypothetical signal. The signal (of an enhanced $W_L^+ W_L^+$ scattering) and the background are more precisely defined in Sec. II. Furthermore, we emphasize that WW scattering with same-sign W's offers the best physics potential for the LHC.

We first present a systematic review of the different mechanisms leading to WW -pair production at the LHC,

both in the same-sign and opposite-sign channels. We justify why and under which conditions the complicated process of WW production in pp collisions can be reduced to general considerations on W_L and W_T emission off a quark line. We then examine the differences between emission and scattering processes of the W bosons of well-defined, longitudinal or transverse polarizations. For quantitative analyses we apply exact matrix element calculations involving the MadGraph generator [13]. We also briefly show that some basic features of W emission can be qualitatively understood within the framework of the effective W approximation (EWA) [14].

In this work, we choose to focus on the purely leptonic W decays in both the same-sign and opposite-sign WW scattering processes. These channels are known as ''gold plated,'' in spite of their low statistics, because of their relatively low background contaminations and experimental purity.

II. SIGNAL AND BACKGROUND DEFINITIONS

Following the well-established ''subtraction method'' [2], we define the signal of the hypothetical enhancement in the production of WW pairs in association with two parton jets in the Higgsless scenario over the the prediction of the Standard Model with a 120 GeV Higgs,

$$\begin{aligned}\text{Signal} = {} & \sigma(pp \to jjWW)|_{\text{higgsless}} \\ & - \sigma(pp \to jjWW)|_{M_h=120\ \text{GeV}}. \end{aligned} \quad (1)$$

We stress again that the Higgless scenario has been chosen merely as our laboratory in the search for the most efficient selection criteria for a signal of an enhancement in the $W_L W_L$ scattering. The signal comes on top of the irreducible background, which is chosen to be

$$\text{Background} = \sigma(pp \to jjWW)|_{M_h=120\ \text{GeV}}. \quad (2)$$

For the calculations in the Higgsless scenario, we make no distinction between removing all Feynman diagrams involving Higgs exchange or setting an inaccessibly large Higgs mass (10^{10} GeV) in the calculation. Furthermore, instead of using any particular unitarization model, for our purpose it is sufficient to assume that the $W_L W_L$ -scattering cross section saturates just before its partial wave amplitudes hit the perturbative unitarity limit at a WW center-of-mass energy around 1.2 TeV and stays constant above this value. Such an assumption defines the practical limiting case for a signal size which is still consistent with all physics principles. Once all the appropriate selection criteria are applied, we find this prescription reduces the signal size by 20%-23%, depending on the selection details, compared to the purely mathematical Higgsless case with no unitarization at all (of course, mostly affected is the most interesting region of large invariant WW masses).

To a good approximation, the signal comes from the scattering of longitudinally polarized W bosons, by far the most sensitive to the electroweak symmetry breaking dynamics. Irreducible background is dominated by the transverse W production.

The cross sections appearing in the definition of the signal and the background must be calculated in a gauge invariant way, including also $O(\alpha^2)$ (pure electroweak [EW]) and $O(\alpha\alpha_S)$ (QCD) diagrams in which two W's are produced but do not interact. As we shall discuss below, QCD effects, in particular, play an important role in the correct calculation of the background.

Both for the signal and for the background we perform a full matrix element calculation of the processes $pp \to jjW^+W^+$ and $pp \to jjW^+W^-$ using the MadGraph generator, followed by leptonic W decay and quark hadronization. The procedure implies that the intermediate state W's are on shell, which in literature is sometimes referred to as the ''production $\times$ decay'' approximation. In particular, diagrams which contribute to the same final state but do not proceed via an intermediate state consisting of a WW pair are here neglected. The W decay is simulated using a private version of PYTHIA 6, which has the appropriate angular distributions for the decays of W_L and W_T implemented. Such modification of the code (in the standard distribution of PYTHIA 6 [15] the W's are decayed isotropically) is vital in order to obtain the correct kinematic distributions of the final-state leptons. To check the validity of the W on shell approximation, a dedicated study was carried out in which special samples of the $pp \to jjW^+W^+ \to jjl^+l^+\nu\nu$ process generated using this method were compared in detail with $pp \to jjl^+l^+\nu\nu$ samples generated with the PHANTOM program [16], without resorting to any ''production $\times$ decay'' approximation.[1] After imposing exactly the same generation cuts on both samples, comparisons of the respective kinematic distributions of the final-state leptons do not reveal large differences, as shown in Fig. 1. An overall uncertainty in the normalization amounting to a few percent is apparent for the EW background, but all lepton kinematics are adequately described. The signal calculated in the W on shell approximation reveals a deficit of events at low invariant masses of the l^+l^+ pair ($M_{ll} < 200$ GeV). However, this kinematic region is of little relevance to the present analysis and, as we will see later, will be almost completely eliminated by the selection criteria. We conclude that the ''production $\times$ decay'' approximation is unlikely to be a source of any significant bias in the results.

We have also cross checked our calculations for the pure EW jjW^+W^- production against the numbers from Table 7 of Ref. [7] that were calculated using VBFNLO and including NLO QCD corrections to the purely electroweak tree-level process. At the level of their ''inclusive'' cuts, for both Higgs boson mass hypotheses of 100 GeV

[1] M. S. is grateful to the authors of Ref. [11] for granting him access to the PHANTOM data samples.

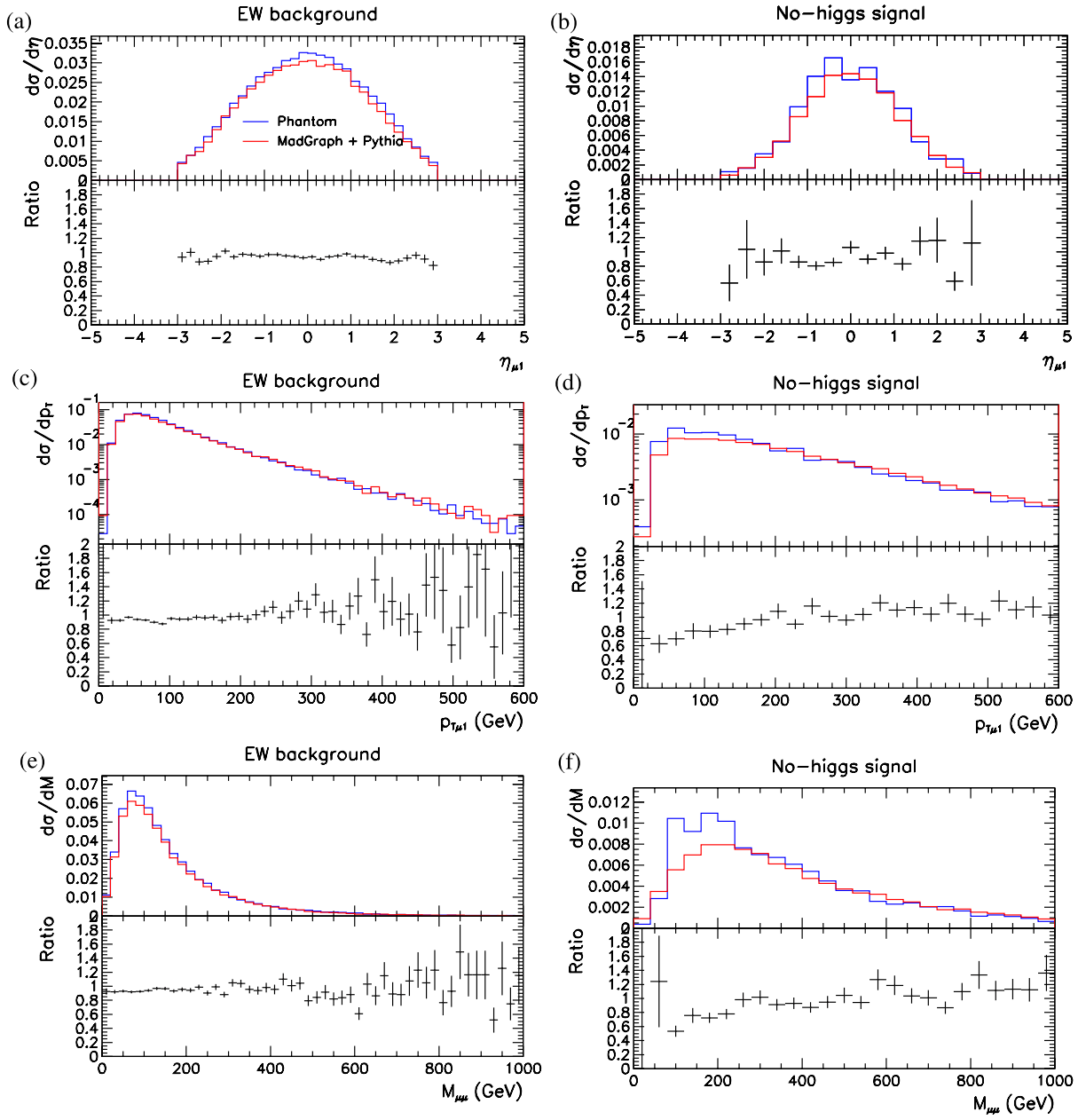

FIG. 1 (color online). Kinematic distributions of final-state muons from the $pp \to jj\mu^+\mu^+\nu\nu$ process at 14 TeV obtained using the W on shell approximation (labeled MadGraph + PYTHIA) and exact matrix element calculations (labeled PHANTOM). The bottom part of each figure shows the ratio MadGraph + PYTHIA/PHANTOM. Pseudorapidities (a), (b); transverse momenta (c), (d); and, invariant masses (e), (f) are shown. For the sake of comparison, background samples contain pure EW processes only and a 200 GeV Higgs is assumed.

and 1 TeV, we find satisfactory agreement, although the agreement in the total cross section expectedly breaks down in the Higgs resonance region.

In the "production × decay" approximation, the signal and the background can be calculated as respective sums over different polarizations of the final WW pairs. Obviously, $W_L W_L$ scattering is very sensitive to the Higgs mass since the Higgs exchange is required to unitarize it. On the other hand, the dependence of the transverse $W_T W_T$ and mixed transverse-longitudinal $W_T W_L$ -pair production on the Higgs boson mass, up to the Higgsless limit, is very weak. We have checked numerically that it less than 3% overall. Therefore, to a good approximation the $W_T W_T$ and $W_T W_L$ contributions in the definition of our signal, Eq. (1), cancel out.

Thus, our effective technical definitions of the signal and background can be rewritten as

$$\text{Signal} = \sigma(pp \to jjW_L W_L)|_{\text{Higgsless}} - \sigma(pp \to jjW_L W_L)|_{M_h = 120\ \text{GeV}}, \quad (3)$$

$$\text{Background} = \sigma(pp \to jjW_L W_L)|_{M_h = 120\ \text{GeV}} + \sigma(pp \to jjW_T W_T) + \sigma(pp \to jjW_T W_L), \quad (4)$$

where each polarization cross section is given in the most general case by a sum of interfering amplitudes: pure electroweak diagrams with interacting and noninteracting WW pairs and QCD-electroweak diagrams with noninteracting WW pairs.

III. W -PAIR PRODUCTION AT THE LHC. EMISSION AND SCATTERING OF LONGITUDINAL AND TRANSVERSE W'S

Production of WW pairs with two associated parton-level jets at the LHC involves hundreds of tree-level diagrams and, in general, is dominated by events with no direct relevance to the mechanism of electroweak symmetry breaking. Signal selection can be crudely divided into two steps: "basic" cuts suppressing the soft parton-parton collisions (both QCD and EW related) leaving mostly events with hard W interactions, and "final" cuts distinguishing the $W_L W_L$ scattering from the irreducible background mainly from $W_T W_T$ and $W_T W_L$ pairs.

The WW -production cross section with polarized W's in the final state can schematically be written as follows:

$$d\sigma_{ij}(M, m_h) = |a(M, m_h)_{ij}\alpha^2 + b(M)_{ij}\alpha\alpha_s|^2, \quad (5)$$

where M is the invariant mass of the WW pair, m_h is either 120 GeV or denotes the Higgsless case, α (α_s) is the electroweak (strong) coupling squared, and subscripts i and j denote the final W -pair polarizations. At the production amplitude level the a-term sums all the pure EW contributions and the b -term comes from a mixed EW/QCD process which is m_h independent. From the above schematic formula the signal defined in Eq. (3) can be written as

$$\text{Signal} \propto \alpha^4[|a(M, \text{Higgsless})_{LL}|^2 - |a(M, m_h = 120)_{LL}|^2] + 2\alpha_s^2\alpha^2\text{Re}[(a(M, \text{Higgsless})_{LL} - a(M, m_h = 120)_{LL})b^\star(M)_{LL}]. \quad (6)$$

From the above one sees that the signal is driven by pure EW processes. The large term $|b_{LL}|^2$ cancels out in the difference through which we define the signal. Moreover, as shown in Fig. 2, QCD events populate mostly a different region of kinematic phase space than the electroweak signal events (mostly apparent in the respective distributions of the W transverse momenta) so interference terms described by the product $[a(p_T^W, \text{Higgsless})_{LL} - a(p_T^W, m_h = 120)_{LL}] \cdot b^\star(p_T^W)_{LL}$ also remain negligibly small compared to the pure EW contribution. This conclusion is valid as much for W^+W^+ as for W^+W^-, even though in the latter case QCD processes dominate the total production rates.

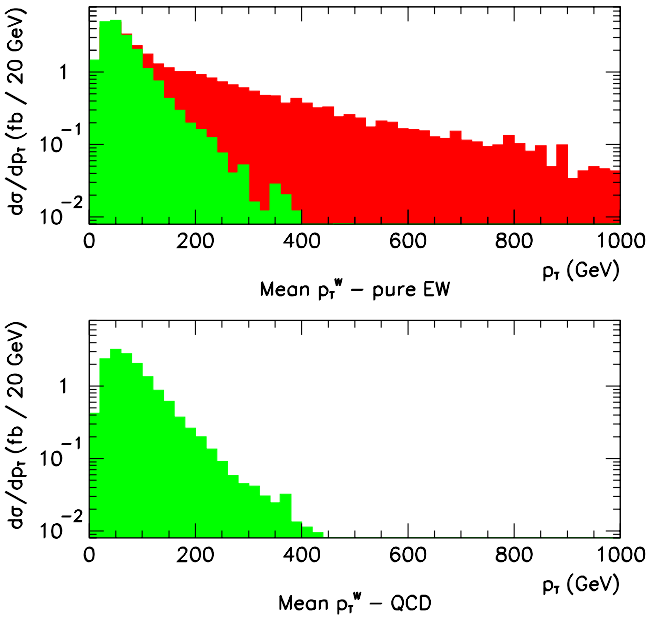

FIG. 2 (color online). Transverse momentum distributions of the W coming from pure EW production (top) and from QCD production (bottom). Electroweak signal, in the sense of Eq. (3), is shown in red (dark grey). Shown in green (light grey) are contributions to the background.

For background that also includes WW bosons with $ij = LT, TT$ polarizations, the effect of QCD processes is much more important since $|b_{ij}|^2$-term is present, and the coherent sum $a_{ij}\alpha$ does not overwhelm $b_{ij}\alpha_s$. In fact, QCD contributions to the total jjW^+W^- production dominate the total cross section by roughly an order of magnitude. In particular, processes involving quark-gluon and gluon-gluon interactions, absent in the same-sign WW channel, here amount to as much as 60% of the total W^+W^- production cross section. For the same-sign WW production, only quark-quark interactions can contribute and QCD effects, in the form of diagrams involving gluon exchange, amount to roughly 50% of the total cross section. Most of these events originate from soft parton-parton collisions (soft partons dominate in the proton PDFs), give very soft kinematics of the accompanying parton jets and can be rejected by appropriate cuts on their rapidity.

Conventional selection criteria for WW scattering processes include the requirement of two tag jets in the forward region and in opposite directions. We will quantify this requirement as

$$2 < |\eta_j| < 5 \quad \text{and} \quad \eta_{j1} \cdot \eta_{j2} < 0, \quad (7)$$

where the η_j denote pseudorapidities of the parton-level jets. Detector acceptance imposes stringent limits on the allowed lepton kinematics to be considered, which at the level of undecayed W can be approximated as a cut on the W pseudorapidity

$$|\eta_W| < 2. \tag{8}$$

The effect of these basic cuts is twofold. As illustrated in Fig. 3, they significantly reduce the irreducible electroweak background coming from low energy parton-parton collisions, that are in the region of small transverse momenta of the parton-level jets. They also reduce the QCD background, to the effect of same-sign WW production being dominated by pure electroweak production.

Ultimately, a full calculation of the same-sign WW production with all the proper EW/QCD interference terms included end up in background rates that are larger by less than 10% compared to a pure EW calculation after all selection criteria are applied, and indeed many previous

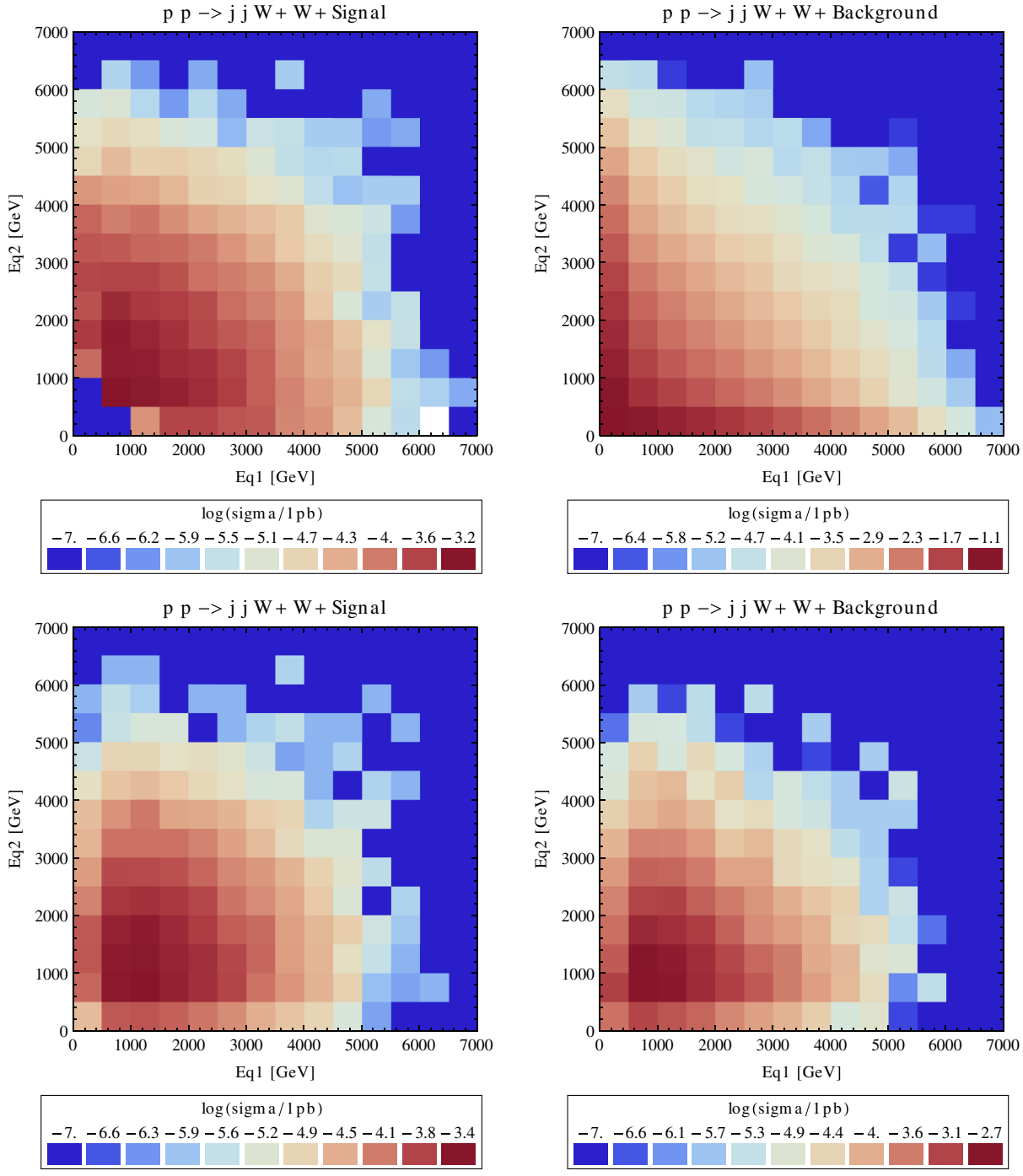

FIG. 3 (color online). Cross section for the $pp \to jjW^+W^+$ process at 14 TeV as a function of incident quark energies. (Left Column) Signal as defined in Eq. (3). (Right Column) Background Eq. (4), upper row: without cuts; lower row: after basic cuts of Eqs. (7) and (8).

studies neglected this contribution altogether. However, the residual QCD contribution to the background in the W^+W^- channel is still sizable, including that from quark-gluon and gluon-gluon interactions and from other processes which change the overall kinematic characteristic of the background for W^+W^-.

In all our MadGraph calculations we use a fixed factorization and renormalization scale of 91.188 GeV. Our QCD cross sections for the process $pp \to jjW^+W^-$ are in agreement to $\sim$10% with the respective numbers from Table 7 of Ref. [7] once their "inclusive" cuts are applied, which may well be taken as the intrinsic uncertainty of our QCD background calculations. It should be noted, however, that unlike the authors of Ref. [7] we compute QCD backgrounds together with EW backgrounds, with all due interference terms in place.

From Fig. 3 we see that basic cuts on the pseudorapidities of parton-level jets and the outgoing W's in the same-sign channel case produce a sample of events with little contamination from low energy quark-quark collisions. For the background this also means little QCD contribution left. At the quark level, the process that dominates same-sign WW production at the LHC is an approximately symmetric quark-quark interaction, with its center-of-mass energy typically peaking at $\sim\sqrt{s}/7$, associated with a W emission from each quark line. Thus, the basic features of $pp \to jjW^+W^+$ at 14 TeV are qualitatively similar to those of a pure quark-level process $uu \to ddW^+W^+$ at an energy of about 2 TeV. Analysis of this much simpler process is helpful in deriving effective criteria to separate the W_LW_L scattering signal from the background that remains after the basic cuts and includes scattering processes with transverse W's.

The characteristic difference in the kinematics of the LL and TT + TL final states in the quark-level process are illustrated in Fig. 4 where the results of a MadGraph simulation of the $uu \to ddW^+W^+$ process at 2 TeV are shown. The longitudinally polarized W tends to be emitted at a smaller angle (hence smaller p_T) with respect to the incoming quark direction than the transversely polarized W [2,17]. As a consequence, the final quark accompanying the longitudinal W is more forward than the one associated with the transverse W. This effect is more pronounced the larger the invariant mass of the WW pair. The p_T distributions of quarks associated with W_L emission become narrower as M_{WW} increases and the peak of the distributions gradually moves to lower values. No such trend is visible for the quarks associated with W_T emission, except for M_{WW} larger than 800 GeV, where the effects of overall energy and momentum conservation become significant.

Those qualitative observations suggest that the higher the invariant mass of the WW pair the easier it becomes the isolation of the longitudinal WW signal from the transverse WW background. Tagging of forward jets at a fixed large value of M_{WW} is the ideal technique to be used.

It is interesting to note that all these features are qualitatively reproduced within the framework of the effective W approximation, where we can identify the signal and the background with W_LW_L and W_TW_T, respectively (Fig. 5).

In pp collisions, the above regularities are at first completely masked by the overwhelming low energy and highly asymmetric quark-quark collisions as well as QCD effects, but become visible again after the basic cuts discussed earlier. This is shown in Fig. 6.

The bounds on η_W (here mimicking cuts on the pseudorapidities of W decay products that are necessary to meet detector acceptance criteria) are instrumental in further reduction of the TT + TL background. As shown in Fig. 7, in an ideal process $WW \to WW$, with two beams of real W's colliding at a fixed energy M_{WW}, the angular distributions of the scattered longitudinal and transverse W's (measured in the WW center-of-mass and with respect to the incoming W direction) become more different with the increase of M_{WW}. The cross sections for WW scattering

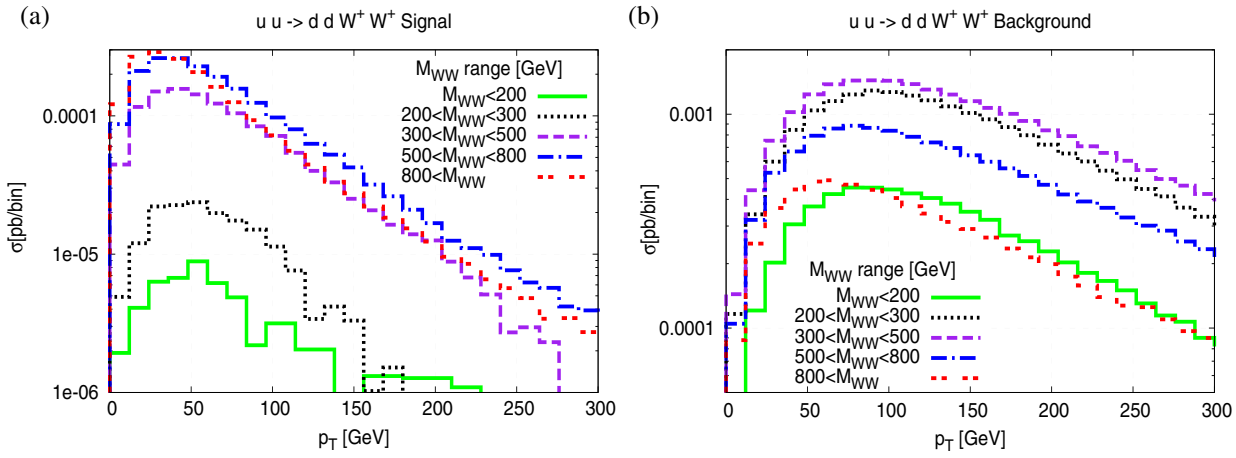

FIG. 4 (color online). p_T distributions of parton-level jets in symmetric quark-quark collisions $uu \to jjW^+W^+$ with initial quarks of 1 TeV energy: (a) signal, (b) background. Results from a MadGraph calculation.

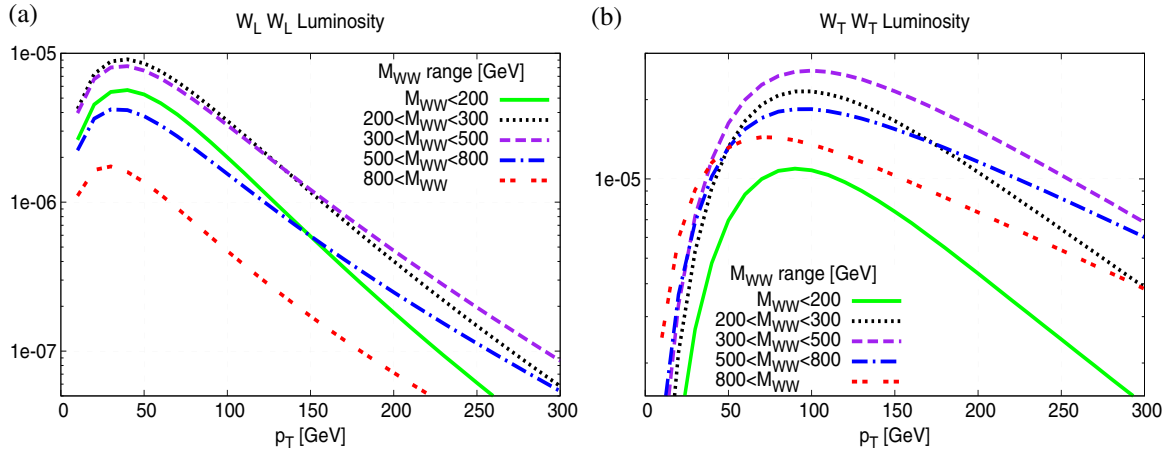

FIG. 5 (color online). p_T distributions of parton-level jets associated with W emission in symmetric quark-quark collisions with initial quarks of 1 TeV energy: (a) for longitudinal W's, (b) for transverse W's. Result (up to an overall normalization factor) of an EWA calculation of the emission probability of two W's, each from a different quark line, for given W helicities and WW invariant mass ranges.

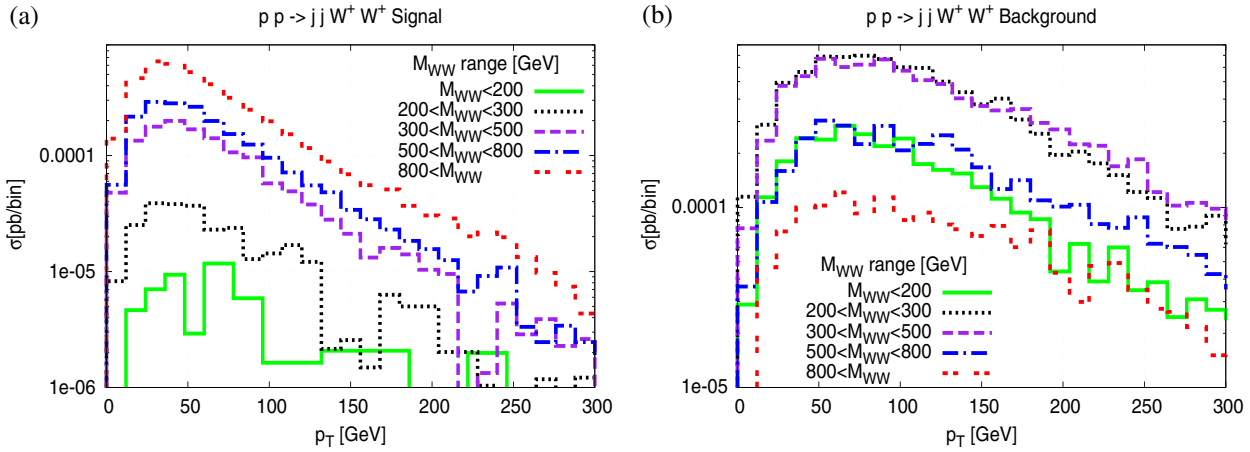

FIG. 6 (color online). p_T distributions of jets in a proton-proton collision $pp \to jjW^+W^+$ with each proton of 7 TeV energy: (a) signal, (b) background, after applying the basic cuts described in the text. Results of a MadGraph calculation.

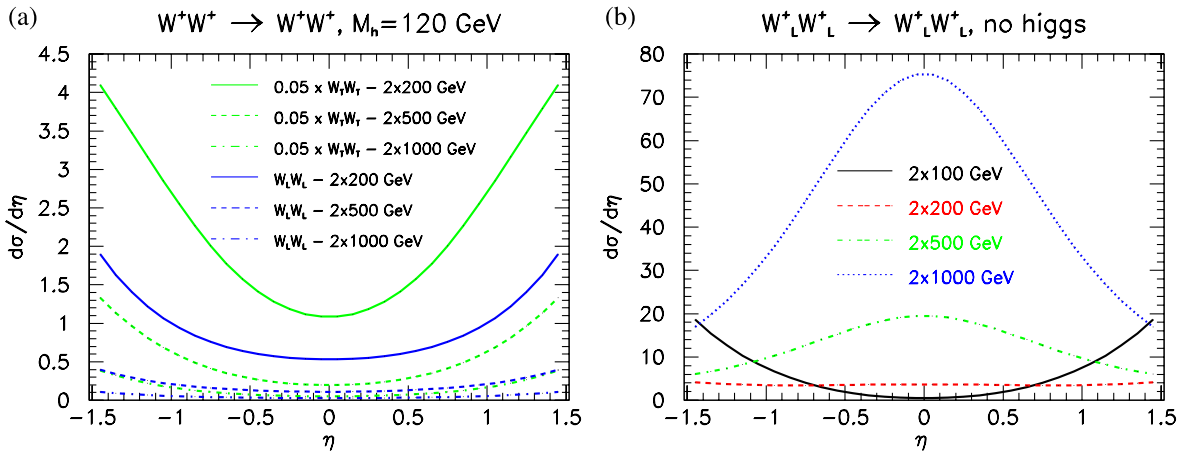

FIG. 7 (color online). Angular distributions of scattered W's with respect to the incoming W direction, in a W^+W^+ scattering process at different center-of-mass energies: (a) in the presence of a 120 GeV Higgs boson, (b) in the no-Higgs case.

with polarization flip, e.g., $W_T W_T \to W_L W_L$, are typically 3 orders of magnitude smaller than the polarization-conserving ones and cannot influence the overall angular characteristics.

As discussed above, jet p_T distributions depend on the emitted W polarization and, in particular, W_T rejection can be improved by requiring smallness of the transverse momenta of both jets. Any Higgsless or non-SM Higgs scenario will modify the angular distributions of outgoing longitudinal W's by making them more central with respect to the incoming W_L direction. Requirement of a large vector boson p_T measured in the lab frame combines the effects of a large W scattering angle and small W emission angle from the parent quark line, both of which favor longitudinal over transverse W's. In search for the most efficient selection criterion that would combine low jet p_T and large vector boson p_T, we notice that in the small $|\eta_W|$ region the M_{WW} value strongly correlates with the product of the two transverse momenta, $p_T^{W1} \cdot p_T^{W2}$. In the leptonic W decay channels, where we do not know the exact kinematics of the two decaying W's, the p_T values of the leptons and, in particular, their product are the best practical measures of M_{WW}. Consequently, a large value of the product $p_T^{l1} \cdot p_T^{l2}$ is an approximate experimental signature of the kinematic region which is most sensitive to the actual mechanism of electroweak symmetry breaking and offers the best capabilities to separate longitudinal from transverse WW scattering processes in any scenario that enhances the $W_L W_L$ cross section for large M_{WW}. Correlation between high $p_T^{l1} \cdot p_T^{l2}$ and high M_{WW} is stronger if one additionally asks for large ratios of p_T^l / p_T^j. For high pseudorapidity jets this means removing events with very large jet energies and little energy left for the W.

The above considerations make it clear that a large value of the following ratio R_{p_T} of the four transverse momenta

$$R_{p_T} = \frac{p_T^{l_1} \cdot p_T^{l_2}}{p_T^{j_1} \cdot p_T^{j_2}}, \tag{9}$$

where l_1 and l_2 denote the two leptons in no particular order, and j_1 and j_2 denote the two most energetic jets in the event is bound to have a large efficiency in isolating hard $W_L W_L$ scattering from the SM background. Such ratio automatically accounts for the correlations that are likely to be satisfied by the signal, but not by the background, and thus work more efficiently than a collection of uncorrelated cuts on the individual variables.

In the rest of the paper we discuss the impact of using the new variable as a selection criterion and the resulting perspectives for the observation of $W_L W_L$ scattering at the LHC. In particular, in Sec. V we compare the selection efficiencies with and without the variable R_{p_T} in the analysis of the same-sign WW channel and demonstrate that the new criterion can significantly improve the (S/B) figures for this process.

The kinematics of signal and background for the opposite-sign channel differs from that of the same-sign channel in several significant ways. Apart from the residual QCD background which softens the average jet p_T and worsens its separation from the signal, pure EW background receives additional contributions from t-channel processes in which both the W^+ and the W^- originate from the same parent quark line. This is another source of softening of the average jet p_T for jets accompanying $W_T^+ W_T^-$ pairs and a class of processes not covered in the EWA approach. On top of that, both signal and background receive contributions from s-channel processes with a $W^+ W^-$ pair being produced from a Z or a Higgs boson. Finally, parton distribution functions also play some role, since the two valence u quarks of the proton favor $W^+ W^+$ production. All these effects change the overall kinematics of the signal and, most importantly, of the irreducible background. In Sec. VI we show that these features indeed reduce the practical usefulness of the R_{p_T} variable in the analysis of the opposite-sign channel.

IV. REDUCIBLE BACKGROUND

Among the many potential sources of reducible background, inclusive $t\bar{t}$ production appears to be most difficult to suppress. Having this background under control is of course most critical in the jjW^+W^- channel where top decays can directly fake the signal. It turns out however that also in the jjW^+W^+ channel due to the huge initial cross section for $t\bar{t}$ production, even tiny detector effects cannot be completely disregarded and can contaminate the signal to measurable amounts, necessary to estimate and subtract. The two main mechanisms for a $t\bar{t}$ pair to fake the same-sign WW scattering signal are: lepton sign misidentification and leptonic B decays.

We have developed and implemented two independent methods to estimate the magnitude of the inclusive top-pair production. The first method relies on an analysis of two separate samples generated with MadGraph: one of $pp \to t\bar{t}$ and another of $pp \to t\bar{t}q$ (top pair production with an associated light quark). Both samples were then processed with PYTHIA to account for the effects of initial- and final-state radiation, top decay, hadronization, and jet formation. Since the respective sets of Feynman diagrams, which are included in the calculation of the two samples are mutually exclusive, the procedure does not involve any event double counting and the events can be simply added at the end. The caveat of this method is that it does not encompass all possible processes leading to top-pair production with one or two additional jets, since diagrams involving gluon emission off an internal quark line are neglected here. However, our cross section calculation for $\sqrt{s} = 7$ TeV gives a total of 198 pb, which is in fair agreement with already published CMS and ATLAS data [18].

In the second method we generate three samples using MadGraph: $pp \to t\bar{t}$, $pp \to t\bar{t}j$ and $pp \to t\bar{t}jj$, with

$j = q, g$, then we likewise use PYTHIA for initial- and final-state radiation, top decay, hadronization, and jet formation. To avoid double counting of the events we follow the prescription described in more detail in Ref. [7], which amounts to selecting from each sample only the events with mutually exclusive topologies. In our case, we keep only events in which the number of b quarks outgoing at a pseudorapidity $2 < |\eta| < 5$ is 2, 1 or 0, respectively. The three samples thus represent the respective lowest-order processes for which 0, 1 or 2 tagging jets arise from gluons or light quarks. This method is formally more complete and coherent, even though the total cross section without cuts cannot be deduced and confrontation with existing experimental data must necessarily rely on comparisons with results obtained from the former method. All the $t\bar{t}$ numbers we will quote in this paper are to be understood as arising specifically from the latter method and having been additionally cross checked with the former.

In the determination of $t\bar{t}$ background we will be assuming throughout this paper an average b-tagging efficiency of 50% for a single b, with a negligible ($\sim 1\%$) probability of mistagging a lighter quark or gluon, in reasonable consistency with recent CMS reports [19].

Determination of background arising from leptonic B decays requires final-state radiation switched on and some jet reconstruction procedure to be adopted. In this work we used the jet reconstruction algorithm which is provided by PYTHIA routine PYCELL, with the cone width set to 0.7. For consistency we also used exactly the same procedure for the irreducible background as well as for the signal. Compared to a pure parton-level analysis, this implies a decrease in the number of accepted signal events by nearly 10%.

The primary selection criteria used to suppress the $t\bar{t}$ background consist of stringent cuts on the invariant mass of the two most energetic jets in the event and combinations of jets with leptons, see Fig. 8. Based on these distributions we chose to apply cuts on the invariant masses of combinations $j_1 l_2$ and $j_2 l_1$ (both jets and leptons are ranked according to their transverse momenta) at 200 GeV. Cuts on the other two jet-lepton combinations are optional, we find however that they do not improve the final figure of merit, defined as $S/\sqrt{S+B}$, and hence we drop them. We also apply a cut on the jet-jet invariant mass whose actual value is subject to individual optimization in each analysis.

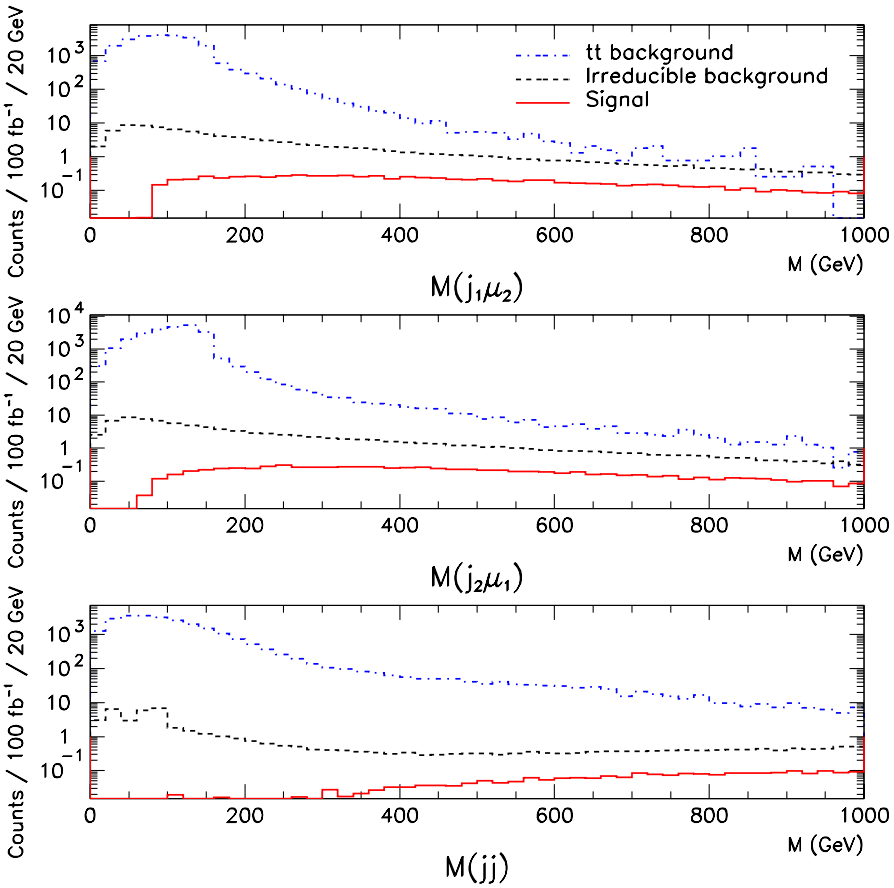

FIG. 8 (color online). Kinematic distributions of the $t\bar{t}$ background compared to signal and irreducible background in the $pp \to jj\mu^+\mu^+\nu\nu$ process at 14 TeV: Invariant masses of two leading jets (bottom) and combinations of jets and muons (top and middle).

Furthermore, in order to estimate some reasonable event yields in the analysis of the same-sign WW channel, we will assume a realistic efficiency of muon sign matching of 99.5% for $p_T \sim 300$ GeV [20]. For electrons at $|\eta| < 2$, a 99% sign matching capability with an overall electron reconstruction efficiency of 95% seems attainable in CMS [21] and these values will be assumed in the rest of the paper.

We have not studied any possible additional sources of reducible background in this work since they have been shown less relevant in both the jjW^+W^+ and jjW^+W^- channels (e.g., [22]) and partly because most of these backgrounds involve various detector effects which cannot be studied without a proper detector simulation. In particular, one should be mindful of the potentially harmful additional reconstruction backgrounds in the electron channel, notably the "fake electron" background, but such considerations surpass the scope of the present work.

V. THE SAME SIGN *WW* CHANNEL

We have generated the following samples: $jjW^\pm W^\pm$ in the SM with a 120 GeV Higgs (accounting for the total irreducible background), $jjW_L^\pm W_L^\pm$ in the SM with a 120 GeV Higgs and in the Higgsless case (for the signal calculation), and several $t\bar{t}$ samples generated as described in the previous section. Generated numbers of events and the respective cross sections, together with other details, are shown further in Tables I and II. The only generation-level cut was $2 < |\eta_j| < 5$ for both outgoing parton-level jets (except for the $t\bar{t}$ samples, where no generation-level cuts were applied), to avoid the most background-dominated kinematical region and satisfy detector acceptance.

The conventional approach to decrease the irreducible background consists of applying a set of uncorrelated leptonic cuts in addition to jet cuts. As discussed in Sec. III, leptons originating from the decay of hard WW scattering processes tend to have larger transverse momenta; they are more central, more back-to-back, and have larger invariant masses than those from background processes. Finally, the bulk of the background from $t\bar{t}$ with a B meson decaying into leptons can be efficiently suppressed by lepton isolation techniques, which we will approximate here with a requirement of no reconstructed jets within a cone of 0.4 centered at each lepton. We also require no tagged b and no additional leptons with $p_T > 10$ GeV within $|\eta| < 2$. A complete set of conventional signal selection criteria can be (set I)

(i) exactly 2 same-sign leptons within detector acceptance,
(ii) 2 tag jets with $2 < |\eta_j| < 5$ and opposite directions,
(iii) no b-tag,
(iv) $M_{j_1 l_2}, M_{j_2 l_1} > 200$ GeV,
(v) $M_{jj} > 400$ GeV,
(vi) $\Delta R_{jl} > 0.4$,
(vii) $p_T^{l_1}, p_T^{l_2} > 40$ GeV,
(viii) $|\eta_{l_1}|, |\eta_{l_2}| < 1.5$,
(ix) $\Delta\phi_{ll} > 2.5$,
(x) $M_{ll} > 200$ GeV.

After adding all the same-sign leptonic channels together ($l^+ = \mu^+, e^+$), we get selection efficiencies and final cross sections as shown in Table I and the l^+l^+ invariant mass of the selected events as shown in Fig. 9(a). Normalized to 100 fb^{-1}, we get a signal-to-background $S/B \approx 11/7$. It should be stressed here that surviving background includes a

TABLE I. Results of conventional selection criteria (I) and new selection criteria (II) for the jjl^+l^+ channel. The signal is the result of subtracting the first row from the second row. "Other reductions" stand for losses due to b tagging, lepton reconstruction and sign matching, respective branching fractions, and the unitarity bound, wherever appropriate.

Sample	Initial σ	Generated events	Selected events (I)	Selected events (II)	Other reductions	Final σ (I)	Final σ (II)
$W_L^+W_L^+$ SM	7.6 fb	56485	534	523	0.0426	0.0031 fb	0.0030 fb
$W_L^+W_L^+$ No Higgs	16.7 fb	56666	11903	12313	0.0335 (I)/0.0329 (II)	0.1117 fb	0.1193 fb
Irreducible background	104.5 fb	170183	1893	855	0.0426	0.0494 fb	0.0224 fb
$t\bar{t}$ background	...	15000000	1805	1318	0.00008	0.0225 fb	0.0171 fb

TABLE II. Results of conventional selection criteria (I) and new selection criteria (II) for the jjl^-l^- channel. The signal is the result of subtracting the first row from the second row. "Other reductions" stand for losses due to b tagging, lepton reconstruction and sign matching, respective branching fractions, and the unitarity bound, wherever appropriate.

Sample	Initial σ	Generated events	Selected events (I)	Selected events (II)	Other reductions	Final σ (I)	Final σ (II)
$W_L^-W_L^-$ SM	1.72 fb	9078	93	94	0.0426	0.0008 fb	0.0008 fb
$W_L^-W_L^-$ No Higgs	4.30 fb	9298	1579	1747	0.0360 (I)/0.0357 (II)	0.0263 fb	0.0288 fb
Irreducible background	20.35 fb	35615	525	241	0.0426	0.0128 fb	0.0059 fb
$t\bar{t}$ background	...	15000000	1805	1318	0.00008	0.0225 fb	0.0171 fb

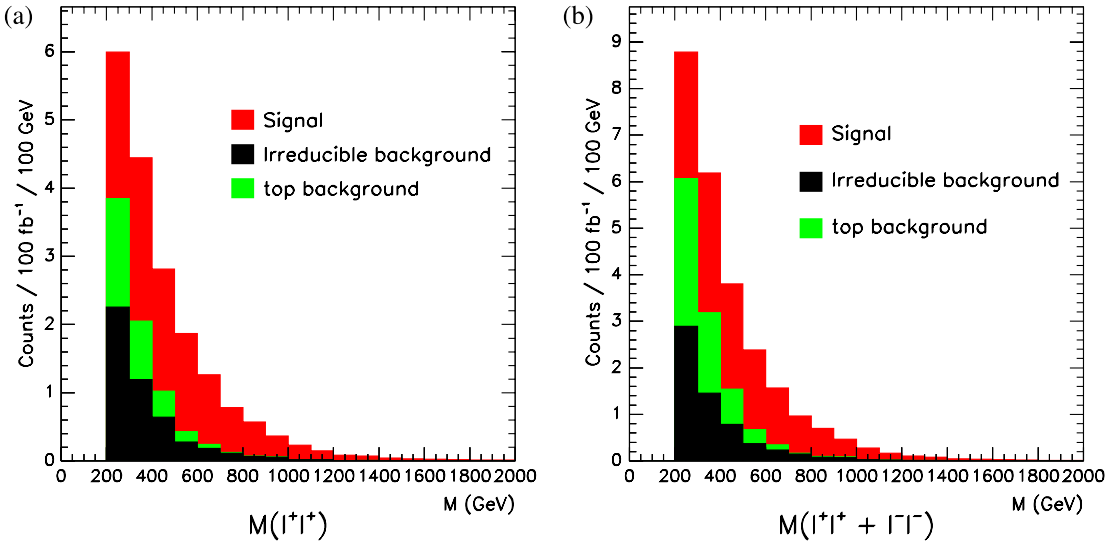

FIG. 9 (color online). Invariant mass distributions of two same-sign leptons after all the conventional signal selection criteria (set I), normalized to 100 fb^{-1}: (a) jjl^+l^+, (b) jjl^+l^+ and jjl^-l^- added.

measurable amount of $t\bar{t}$ and that its dominant source at this point is lepton sign misidentification. The inclusion of the W^-W^- channel provides an additional 25% to the signal and irreducible background (see Table II), but at the same time the $t\bar{t}$ background doubles, ending up in $S/B \approx 13/11$. The corresponding ll invariant mass distribution is shown in Fig. 9(b). Although our set of cuts is not very fine-tuned, it already produces a result which is roughly comparable with previous analyses in the same-sign lepton channel, in particular, with the recent Ref. [5]. Several differences exist between the two analyses (in order of relevance: no $t\bar{t}$ background included, no unitarity limit applied in the no-Higgs case, cuts done on parton-level variables, different treatment of QCD background, and a different default Higgs mass). Recalculating under their assumptions, our result translates into $S/B \approx 17/7$ per 100 fb^{-1}, to be compared with their best result $S/B = 13/6$[2] (for a discussion of the differences, see Sec. VII).

In Sec. III we proposed a new variable R_{p_T} that gives a direct signature of a hard $W_L W_L$ scattering process and that replaces the conventional cuts. We thus now go back to the point where only generation-level cuts and $t\bar{t}$ cuts have been applied and study the correlations between the transverse momenta of the W bosons and the jets for those signal and background events which survived those cuts. This is shown in Figs. 10(a) and 10(b). It is apparent that a line corresponding to a constant ratio

$$p_T{}^{W_1}/p_T{}^{j_1} \cdot p_T{}^{W_2}/p_T{}^{j_2} = 12 \tag{10}$$

has indeed a large discriminating power between signal and background, leaving the bulk of the background above, while keeping a substantial part of the signal below. In Fig. 10(c) the same correlations are shown for the transverse momenta of the outgoing leptons instead of the W's. Although W decay tends to smear this nice picture out (it is of course very important to take proper account of the correct angular distributions of W decays according to the different helicities in signal and background, but these differences unfortunately do not play any positive role in isolating signal from background), the interesting observation is that the outgoing leptons from W decay sufficiently keep the basic kinematic features characteristic for signal and background of their parent W's. Consequently, a line of constant ratio

$$R_{p_T} = 3.5 \tag{11}$$

still has a remarkably large discriminating power between signal and background. This is illustrated in Fig. 10(d), where the upper plot shows the ratio of signal-to-background and in the lower plot the R_{p_T} distributions for signal and background are given. When applied on top of all the remaining selection criteria, the efficiency of a cut that requires R_{p_T} be larger than 3.5 is 0.77 for the signal and 0.14 for the background, which makes it more effective than all the alternative conventional cuts taken together.

Thus, our complete set of selection criteria is now (set II)

(i) 2 same-sign leptons,
(ii) 2 tag jets with $2 < |\eta_j| < 5$ and opposite directions,
(iii) no b-tag,
(iv) $M_{j_1 l_2}, M_{j_2 l_1} > 200$ GeV,
(v) $M_{jj} > 500$ GeV,
(vi) $R_{p_T} > 3.5$,
(vii) $\Delta\phi_{ll} > 2.5$.

[2]To derive this number, we take the row corresponding to $M_{\text{cut}} = 400$ GeV from Table 4 of Ref. [5], treat the "$M_H = 200$ GeV" cross section as the irreducible background and subtract it from the "no Higgs" cross section to get the signal, then normalize the result to 100 fb^{-1}.

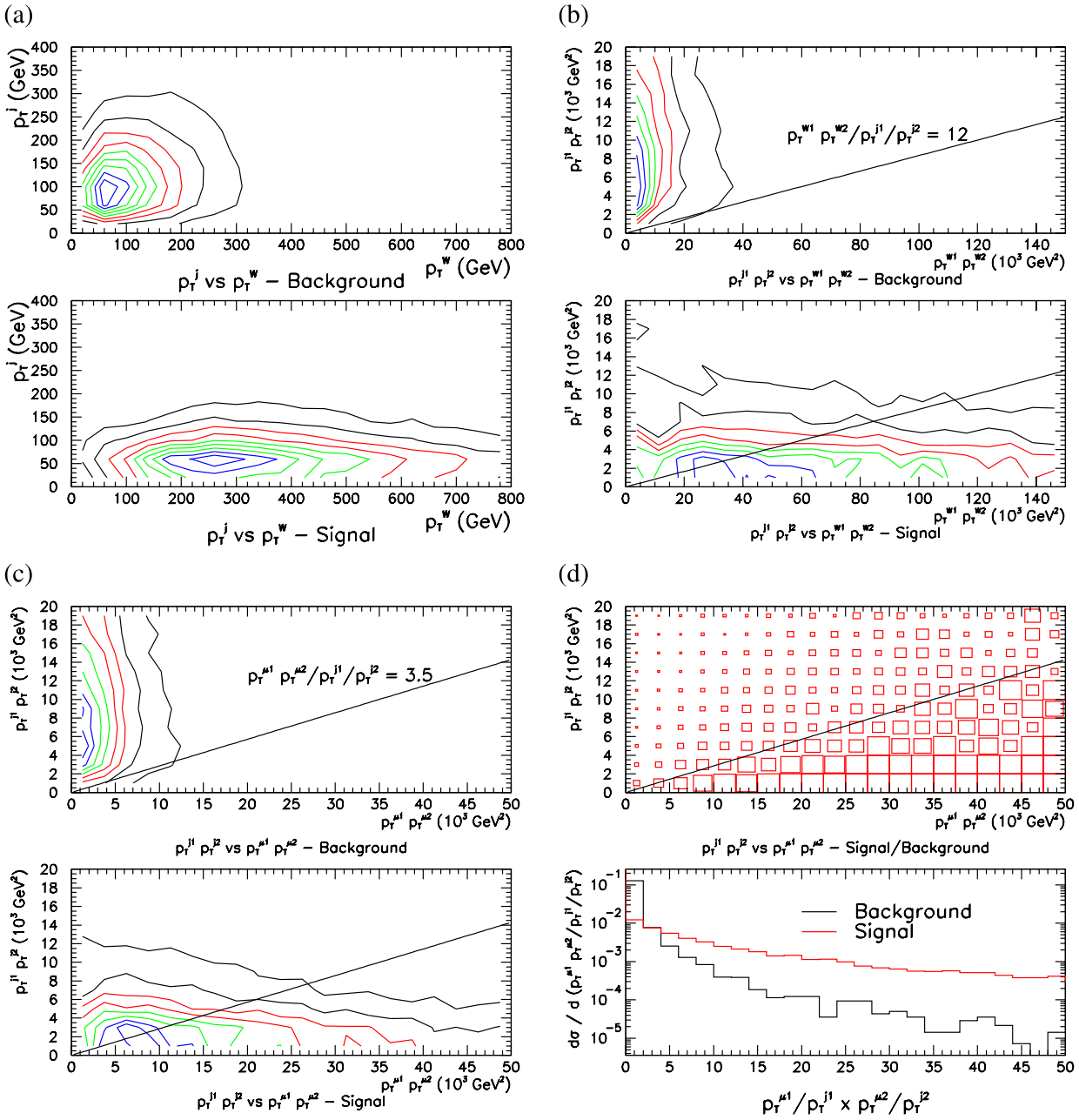

FIG. 10 (color online). Transverse momenta and their combinations for signal and for the irreducible background in the jjW^+W^+ channel at 14 TeV, after applying the cuts against top production: (a) individual p_T of W's and jets, (b) p_T products of two W's and two jets, (c) p_T products of two leptons and two jets, and (d) the signal-to-background ratio (top) and the R_{p_T} distribution for the signal and for the background (bottom). Contours in (a) through (c) represent the lines of constant cross section, with values increasing linearly from the outermost (black) to the innermost (blue) contours. Each plot is normalized to its own maximum value.

Note that a combination of only the last two cuts allows the release of several other selection criteria that are conventionally used to cope with the irreducible background. The R_{p_T} cut also automatically removes the $t\bar{t}$ background related to leptonic B decay to a negligible level, hence we are free to drop any lepton isolation or central jet veto cut, which may well prove an advantage in a high pileup regime like the LHC. Here we have also modified the M_{jj} cut to a higher value, since we find such change produces an improvement in combination with the R_{p_T} cut, but not in combination with the conventional cuts.

A summary of results obtained with the conventional cuts (set I) and the R_{p_T} cut (set II) is shown in Tables I and II. For an easy comparison of both results, the selection criteria were chosen such as to keep in both cases a similar

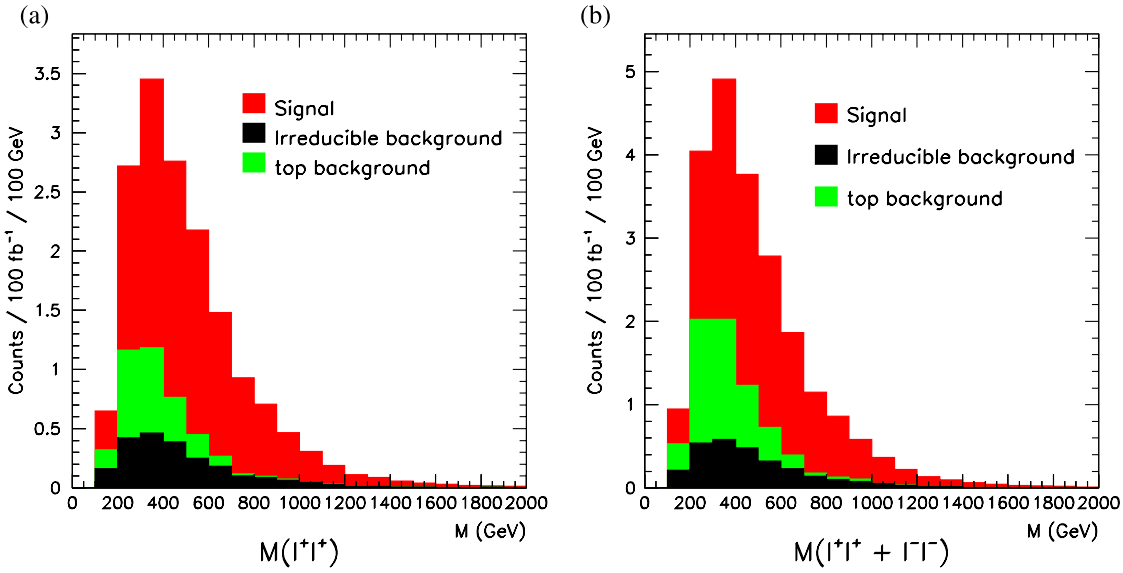

FIG. 11 (color online). Invariant mass distributions of two same-sign leptons after all the new signal selection criteria (set II), normalized to 100 fb^{-1}: (a) jjl^+l^+, (b) jjl^+l^+ and jjl^-l^- added.

amount of signal. Relative to the amount of signal, we find the R_{p_T} cut improves rejection power against the irreducible background by a factor 2.5 and against the $t\bar{t}$ background by about 1/3. Figure 11(a) and 11(b) show the corresponding invariant mass distributions of the two same-sign leptons for this case (to be compared with respective plots in Fig. 9). We arrive at $S/B \approx 12/4$ once all the l^+l^+ channels are summed up and $S/B \approx 14/6$ by additionally including the l^-l^- channels.

It is interesting to note that R_{p_T} being a dimensionless number does not depend on $\sqrt{s}$ to first approximation. In principle, exactly the same cut could be also used in an analysis of pp data at 7 TeV or at 8 TeV. The efficiency of such a cut (calculated on top of all the other cuts) at $\sqrt{s} = 7$ TeV (8 TeV) is 0.71 (0.72) for the signal and 0.12 (0.12) for the irreducible background, which is only slightly weaker than for $\sqrt{s} = 14$ TeV. It is mainly due to the much lower signal cross section to begin with (factor $\sim$7 at the level of generation cuts) that 7 TeV or 8 TeV ultimately does not offer the possibility to observe the signal in a viable amount of time. However, the efficiency of the R_{p_T} variable can be experimentally tested at 7 TeV or 8 TeV.

VI. THE OPPOSITE-SIGN WW CHANNEL

As already stated in Sec. III, due to the many additional contributions to the background in the jjW^+W^- channel (both in terms of Feynman diagrams and physical processes), there is good reason to expect a lower R_{p_T} efficiency. In this section we present our own analysis of the jjW^+W^- channel for the sake of a direct comparison. Generated samples, initial and final cross sections for the signal and for the backgrounds are shown in Table III. Cuts imposed at the generation level were

(i) $|\eta_j| < 5$,
(ii) $\Delta\eta_{jj} > 4$,
(iii) $p_T^j > 10$ GeV,
(iv) $M_{jj} > 350$ GeV.

An attempt to exploit the kinematic correlations between W's and jets and between leptons and jets, in a similar manner as was applied for the same-sign channel and presented in Sec. V, is shown in Fig. 12. Many important differences with respect to the same-sign channel are readily visible. First and foremost, background extends to much lower jet transverse momenta, to the effect of background

TABLE III. Results for the jjl^+l^- channel. The signal is the result of subtracting the first row from the second row. "Other reductions" stand for losses due to b tagging, lepton reconstruction, respective branching fractions, and the unitarity bound, wherever appropriate.

Sample	Initial σ	Generated events	Selected events	Other reductions	Final σ
$W_L^+W_L^-$ EW SM	24.9 fb	90296	777	0.0426	0.0091 fb
$W_L^+W_L^-$ EW No Higgs	44.0 fb	102570	8257	0.0362	0.1282 fb
Irreducible background	3.37 pb	500000	458	0.0426	0.1315 fb
$t\bar{t}$ background	...	15000000	194	0.0028	0.3610 fb

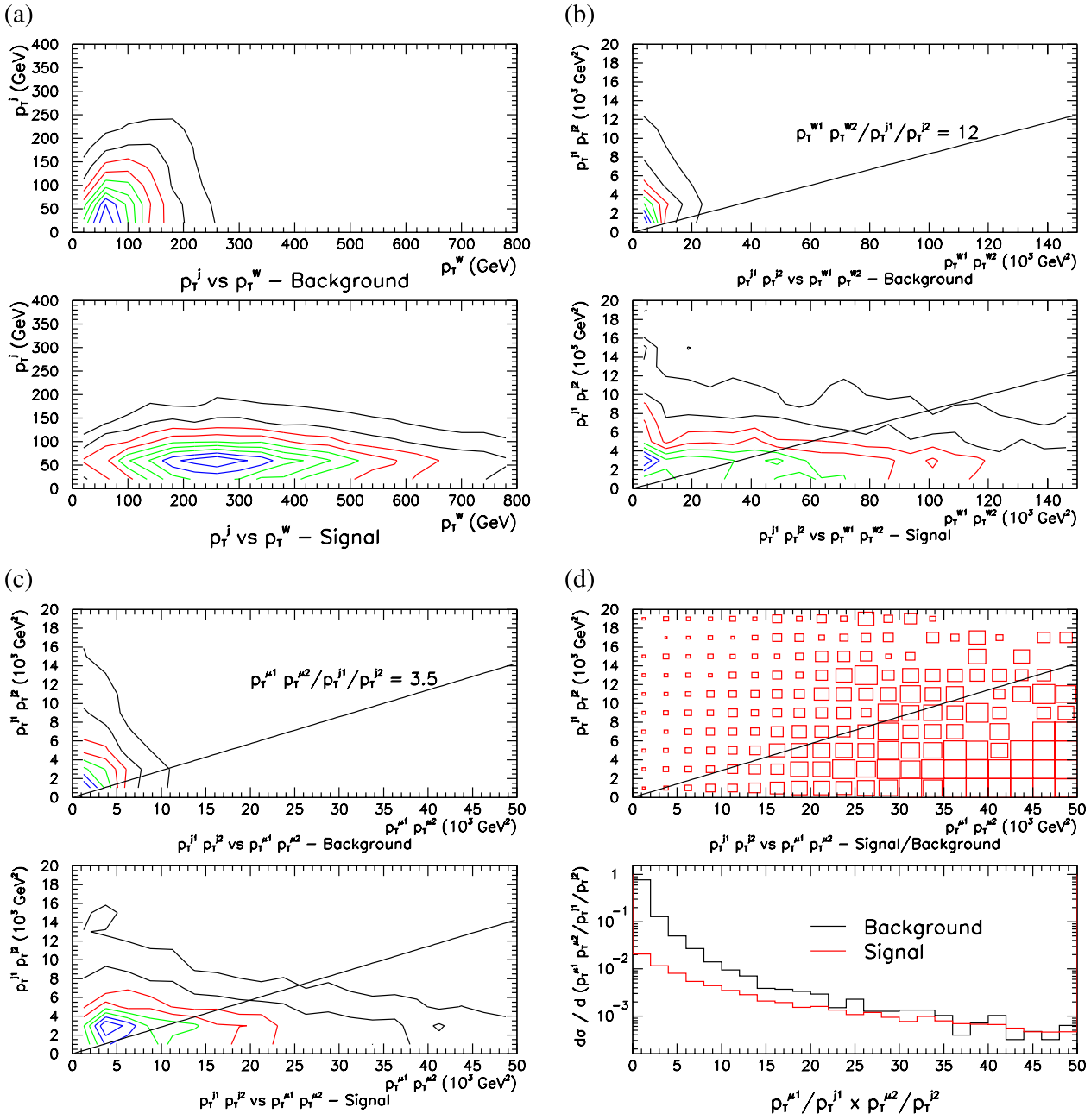

FIG. 12 (color online). Transverse momenta and their combinations for signal and for the irreducible background in the jjW^+W^- channel at 14 TeV, after applying the cuts against top production: (a) individual p_T of W's and jets, (b) p_T products of two W's and two jets, (c) p_T products of two leptons and two jets, and (d) the signal to background ratio (top) and the R_{p_T} distribution for the signal and for the background (bottom). Contours in (a) through (c) represent the lines of constant cross section, with values increasing linearly from the outermost (black) to the innermost (blue) contours. Each plot is normalized to its own maximum value.

and signal being marginally distinguishable in the jet p_T distributions [Figs. 12(a) and 12(b)]. In these circumstances, the R_{p_T} ratio can only be as effective in separating signal from background as lepton transverse momenta on their own. Figure 12(d) confirms that no particular cut on R_{p_T} can bring background levels below or even close to the signal level without risking very low efficiency. This study concludes that R_{p_T} cannot be used as an effective discriminant. Larger initial cross sections for the signal are unfortunately coupled with a weaker kinematic separation from the background in p_T^l [see Fig. 12(c)]. However, we find the sum $p_T^{l_1} + p_T^{l_2}$, or the product $p_T^{l_1} \cdot p_T^{l_2}$, still has a slightly larger efficiency than combined cuts on the individual p_T^l. Another important disadvantage is that top production can directly fake the signal signature here, rather than being restricted to small experimental effects, and an additional central jet veto is necessary to

bring this background down to a manageable level. A veto on additional jets with $p_T > 25$ GeV and η anywhere between η_{j1} and η_{j2} removes nearly 75% of the surviving $t\bar{t}$ events at the expense of an additional 15% of the signal.

As usual, we require no tagged b and no additional leptons with $p_T > 10$ GeV within $|\eta| < 2$. Finally, our full selection criteria are

(i) exactly 2 opposite-sign leptons within detector acceptance,
(ii) 2 tag jets with $2 < |\eta_j| < 5$ and opposite directions,
(iii) no b-tag,
(iv) $M_{j_1 l_2}, M_{j_2 l_1} > 200$ GeV,
(v) $M_{jj} > 500$ GeV,
(vi) central jet veto,
(vii) $p_T^{l_1} + p_T^{l_2} > 300$ GeV,
(viii) $\Delta\phi_{ll} > 2.5$,
(ix) $M_{ll} > 300$ GeV.

The result (see Table III) is consistent with those of previously published analyses on the same channel [5,7] (taking into account all the differences in the respective analysis approaches), but does not bring much improvement to the subject.

VII. DISCUSSION AND OUTLOOK

We have presented a detailed phenomenological analysis of WW scattering at the LHC, which in some aspects contains improvements with respect to the analyses published by other authors. Our analysis was optimized primarily for observing a signal of an enhanced $W_L W_L$ scattering at the LHC running at an energy of 7, 8, and 14 TeV. Such an enhancement exists in various theoretical scenarios of the electroweak symmetry breaking (EWSB). It has not been the purpose of this paper to compare different theoretical scenarios but merely to find an improvement in the selection of the signal of the $W_L W_L$ scattering. As a laboratory in our search we have chosen for our hypothetical enhanced $W_L W_L$ scattering the Higgsless scenario, which gives the strongest but physically still realistic enhancement compared to the SM prediction with a light Higgs boson. The discrimination is based essentially on a counting experiment in which a light SM-like Higgs boson as the only source of EWSB should ideally produce an almost null result.

It is not the aim of this work to fine-tune the selection in order to produce the best possible S/B, as the exact criteria will change anyway once a full detector simulation is included. Regardless of that it seems clear that the R_{p_T} variable is able to provide some new insight into the subject and possibly improve the expected performance in the same-sign WW channel. Our result with conventional cuts is roughly consistent with previously published results of similar analyses, in particular with the recent Ref. [5], if the same conditions and assumptions are applied in both cases. Their best result $S/B = 13/6$ is the equivalent of our $S/B \approx 17/7$ per 100 fb^{-1}. In fact, most of the difference comes from the fact that their analysis includes a cut on the minimum jet p_T at 30 GeV which is the standard in LHC experiments, but very costly to the signal as far as $W_L W_L$ selection at high invariant mass is concerned. With the R_{p_T} cut instead this result could become even $S/B \approx 17/3$.

The question of a practical minimum jet p_T cut, in particular having in view the large LHC pileup, is an issue that requires a careful dedicated study which is clearly beyond the scope of the present work. In this paper we show a strong physics motivation for releasing the stringent cuts on jet p_T (our analysis implicitly assumes $p_T > 10$ GeV, i.e., jets below that threshold are not reconstructed). The idea of tagging only one forward jet with $p_T > 30$ GeV, which should be rather safe, and working out additional criteria to identify correctly its softer companion, is an interesting possibility that needs to be investigated. Data collected in 2012 may already shed some light on the issue.

Our new selection criterion provides potential to improve the final figure of merit regardless of any working assumptions or approximations we have done throughout this paper. It is clear, however, that many important unknowns still remain and will require a careful experimental study. One is the vulnerability of R_{p_T} to experimental smearing in the measurement of all the individual p_T's. Since R_{p_T} is expected to work for 7 TeV or 8 TeV nearly as efficiently as for 14 TeV, the practical effects of p_T smearing can be studied at the LHC on 2012 data and reasonably assumed not to be worse for future 14 TeV data.

Top background poses more unknowns. The total cross section for top production at 14 TeV will ultimately have to be measured. Since $t\bar{t}$ background to the W^+W^+ channel arising from lepton sign misidentification is not completely negligible, the practical profits from using the R_{p_T} variable will depend on precise knowledge of the sign matching efficiencies of the individual detectors (for demonstration purposes we could of course tune the selection so to kill $t\bar{t}$ completely, but such procedure would also end up in very low signal and hence is of little practical interest). One should note that an important cross check of the $t\bar{t}$ background evaluation can be obtained by comparing the results of the two in principle separate measurements that this analysis involves: the jjl^+l^+ channel and the jjl^-l^- channel. Since the relative amounts of WW in the two channels are like 4:1 and the amounts of $t\bar{t}$ like 1:1, the actual ratio will shed some light on the true composition of the sample. With enough data having been collected, the jjl^-l^- channel could be even used to estimate the remaining $t\bar{t}$ background and subtract it.

Certainly it will be crucial to include the electron channels in addition to the experimentally purest muon channels, as the latter alone do not guarantee enough statistical significance. A further, more detailed study based on a full

detector simulation and detector-specific event reconstruction is vital for the good understanding of rejection capabilities of the detector backgrounds and the resulting purity of electron reconstruction.

Overall, results presented in this paper show that there is good chance to get some important hints about the mechanism of electroweak symmetry breaking already after the first 100 fb^{-1} of data at 14 TeV, by focusing on the purely leptonic W decay channels. We advocate the importance of the same-sign WW channel as the most promising one, particularly in the absence of low mass resonances (1-2 TeV) in the W^+W^- channel.

ACKNOWLEDGMENTS

This work has been supported in part by the Polish Ministry of Science and Higher Education as research projects 666/N-CERN/2010/0, N N202 230337 (2009-12), and N N202 103838 (2010-12) and by the Collaborative Research Center SFB676/1-2006 of the DFG.

[1] G. F. Giudice, C. Grojean, A. Pomarol, and R. Rattazzi, J. High Energy Phys. 06 (2007) 045; K. Cheung, C.-W. Chiang, and T.-Ch. Yuan, Phys. Rev. D **78**, 051701 (2008), and references therein.

[2] J. Bagger, V. Barger, K. Cheung, J. Gunion, T. Han, G. A. Ladinsky, R. Rosenfeld, and C. P. Yuan, Phys. Rev. D **49**, 1246 (1994); **52**, 3878 (1995).

[3] A. Dobado, M. J. Herrero, J. R. Pelaez, E. Ruiz Morales, and M. T. Urdiales, Phys. Lett. B **352**, 400 (1995); Phys. Rev. D **62**, 055011 (2000); J. M. Butterworth, B. E. Cox, and J. R. Forshaw, Phys. Rev. D **65**, 096014 (2002); A. Alboteanu, W. Kilian, and J. Reuter, J. High Energy Phys. 11 (2008) 010; M. S. Chanowitz and W. B. Kilgore, Phys. Lett. B **322**, 147 (1994); **347**, 387 (1995).

[4] E. Accomando, A. Ballestrero, S. Bolognesi, E. Maina, and C. Mariotti, J. High Energy Phys. 03 (2006) 093; A. Ballestrero, G. Bevilacqua, and E. Maina, J. High Energy Phys. 05 (2009) 015; A. Ballestrero, G. Bevilacqua, D. B. Franzosi, and E. Maina, J. High Energy Phys. 11 (2009) 126.

[5] A. Ballestrero, D. B. Franzosi, and E. Maina, J. High Energy Phys. 06 (2011) 013.

[6] B. Jäger, C. Oleari, and D. Zeppenfeld, J. High Energy Phys. 07 (2006) 015; Phys. Rev. D **80**, 034022 (2009).

[7] C. Englert, B. Jäger, M. Worek, and D. Zeppenfeld, Phys. Rev. D **80**, 035027 (2009).

[8] B. Jäger and G. Zanderighi, J. High Energy Phys. 11 (2011) 055; T. Melia, P. Nason, R. Rontsch, and G. Zanderighi, J. High Energy Phys. 11 (2011) 078; T. Melia, K. Melnikov, R. Rontsch, and G. Zanderighi, Phys. Rev. D **83**, 114043 (2011); T. Melia, K. Melnikov, R. Rontsch, and G. Zanderighi, J. High Energy Phys. 12 (**2010**) 053; T. Melia, P. Nason, R. Rontsch, and G. Zanderighi, Eur. Phys. J. C **71**, 1670 (2011).

[9] T. Han, D. Krohn, L.-T. Wang, and W. Zhu, J. High Energy Phys. 03 (2010) 082.

[10] ATLAS Collaboration, arXiv:0901.0512v4.

[11] N. Amapane *et al.*, CMS Analysis Note, Report No. CMS AN-2007/005.

[12] R. Contino, Ch. Grojean, M. Moretti, F. Piccinini, and R. Rattazzi, J. High Energy Phys. 05 (2010) 089; A. Ballestrero, D. Buarque Franzosi, L. Oggero, and E. Maina, J. High Energy Phys. 03 (2012) 031.

[13] J. Alwall, M. Herquet, F. Maltoni, O. Mattelaer, and T. Stelzer, J. High Energy Phys. 06 (2011) 128.

[14] R. N. Cahn and S. Dawson, Phys. Lett. B **136**, 196 (1984); **138**, 464(E) (1984); S. Dawson, Nucl. Phys. **B249**, 42 (1985); G. L. Kane, W. W. Repko, and W. B. Rolnick, Phys. Lett. B **148**, 367 (1984).

[15] T. Sjöstrand, S. Mrenna, and P. Skands, J. High Energy Phys. 05 (2006) 026.

[16] A. Ballestrero, A. Belhouari, G. Bevilacqua, V. Kashkan, and E. Maina, Comput. Phys. Commun. **180**, 401 (2009).

[17] S. Dawson, Phys. Lett. B **217**, 347 (1989).

[18] CMS Collaboration, Phys. Lett. B **695**, 424 (2011); ATLAS Collaboration, Phys. Lett. B **707**, 459 (2012); Y. Okumura, arXiv:1108.6273.

[19] CMS Collaboration, CMS Physics Analysis Summary, Report No. CMS PAS BTV-09-001.

[20] CMS Collaboration, Report No. JINST 5 T03022, 2010

[21] W. Adam *et al.*, CMS Analysis Note, Report No. CMS AN-2009/164.

[22] B. Zhu, P. Govoni, Y. Mao, C. Mariotti, and W. Wu, Eur. Phys. J. C **71**, 1514 (2011).